Near-infrared fluorescence imaging with indocyanine green in vascular surgery

Hoven, P. van den

Chapter 3

Perfusion parameters in near-infrared fluorescence imaging with indocyanine green: a systematic review of the literature

P. van den Hoven [1*], L.N. Goncalves [1*], J. van Schaik [1], L. Leeuwenburgh [1], C.H.F. Hendricks [1], P.S. Verduijn [1], K.E.A. van der Bogt [1], C.S.P. van Rijswijk [1], A. Schepers [1], A.L. Vahrmeijer [1], J.F. Hamming [1], J.R. van der Vorst [1]

1. Leiden University Medical Center, Leiden, The Netherlands

* Authors contributed equally and share first authorship

Published in Life, May 2021.

Abstract

Introduction

Near-infrared fluorescence imaging is a technique capable of assessing tissue perfusion and has been adopted in various fields including plastic surgery, vascular surgery, coronary arterial disease, and gastrointestinal surgery. While the usefulness of this technique has been broadly explored, there is a large variety in the calculation of perfusion parameters. In this systematic review, we aim to provide a detailed overview of current perfusion parameters, and determine the perfusion parameters with the most potential for application in near-infrared fluorescence imaging.

Methods

A comprehensive search of the literature was performed in Pubmed, Embase, Medline, and Cochrane Review. We included all clinical studies referencing near-infrared perfusion parameters.

Results

A total of 1511 articles were found, of which, 113 were suitable for review, with a final selection of 59 articles. Near-infrared fluorescence imaging parameters are heterogeneous in their correlation to perfusion. Time-related parameters appear superior to absolute intensity parameters in a clinical setting.

Conclusion

This literature review demonstrates the variety of parameters selected for the quantification of perfusion in near-infrared fluorescence imaging.

Introduction

Near-infrared fluorescence (NIRF) imaging is a promising technique for visualizing tissue perfusion. The measurement of fluorescence in the near-infrared spectrum is feasible for perfusion assessment due to the low tissue auto-fluorescence in this range. This allows for visualisation of an intravenously-administered fluorophore. The most frequently used fluorescent dye in perfusion assessment is indocyanine green (ICG), which is primarily contained in the vascular system due to its selective binding with the plasma protein albumin. NIRF imaging is minimally invasive, with low risk of side-effects. The use of NIRF imaging as a technique to assess tissue perfusion has been explored in various surgical fields. In plastic surgery this technique has been used to assess perfusion in flap surgery, nipple-sparing mastectomies, and reconstructive microsurgery (1). NIRF imaging has been applied in endocrinological surgery, assisting in the preservation of critical structures, such as the parathyroid gland, during surgical procedures. For patients with peripheral arterial disease (PAD), NIRF imaging can be used for the assessment of regional tissue perfusion. Described applications of NIRF imaging in patients with PAD include (1) diagnosis, (2) the measuring of the effect of revascularization procedures, and (3) the assessment of tissue viability following amputation surgery (2). In cardiac interventions, the use of NIRF imaging has allowed for the real-time assessment of graft patency, with applications in transplantation surgery providing a diagnostic tool for the assessment of kidney microperfusion, for example (3). NIRF imaging has furthermore been applied in neurosurgery, quantifying cerebral perfusion both intra- and postoperatively. In gastro-intestinal surgery, NIRF imaging has been used to assess anastomotic perfusion after bowel resection (4).

To date the perfusion patterns visualized with fluorescence imaging have been quantified using time-intensity curves, from which various parameters can be extracted for statistical analysis. This article will systematically review the literature on the time-intensity curve parameters following NIRF imaging in perfusion assessment, with the aim of identifying optimal perfusion parameters for standardised quantification of perfusion using NIRF imaging.

Methods

Search Strategy

An electronic search was conducted using Pubmed, Medline, Embase and Cochrane Review from inception to January 2021 to identify all relevant literature. Medical Subject Headings (MeSH) were adopted and included: “perfusion”, “near-infrared fluorescence imaging”, and “indocyanine green”. The search strategies applied can

be found in Appendix A. A manual search of references of included articles was also performed to identify further studies of interest. Articles were systematically screened with a two-stage method, with stage one including screening of the title and abstract, followed by stage two with full-text screening. The systematic review of the literature and results conducted in this article are not part of a registered study.

Article selection

Only full-text articles in English were included. Articles reporting the use of fluorescence imaging in animal studies were excluded. Article selection was performed by two independent researchers (L.G. and P.H.). Any article discussing the analysis of tissue perfusion using near-infrared fluorescence imaging was included if fluorescence–intensity curves and perfusion parameters were mentioned. Articles reporting the qualitative use of NIRF imaging without quantitative data were excluded. NIRF perfusion imaging has been applied in numerous surgical fields. The results obtained are therefore divided by subspecialization, which included gastrointestinal, neurological, vascular, transplantation, and plastic surgery, as well as other surgical subspecializations.

Quality assessment. The quality and the risk of bias of the selected and included articles were independently evaluated by two reviewers (L.G. and P.H.) according to the revised Quality Assessment of Diagnostic Accuracy Studies (5). In instances of discrepancy in interpretation, a third independent reviewer (JV) was asked to adjudicate.

Data extraction. Data extracted from all articles reviewed for inclusion consisted of relevant patient characteristics, type of NIRF imaging camera, the ICG concentration, and the perfusion parameters selected.

Results

An overview of the article selection process for this systematic review is reported in a flow diagram in Figure 1, according to the Preferred Reporting Items for Systematic review and meta-analysis Protocols 2015 guidelines. A total of 1511 articles were found based on the search terms in Appendix A, of which 113 were suitable for review, with a final selection of 57 articles. Manual review of the references in the above selected articles lead to the inclusion of 2 further references, providing a total of 59 articles for final inclusion. The results of the quality assessment can be found in the Appendices B and C. The 59 studies selected included a total of 2336 patients. The number of patients in the studies ranged from 1 to 181. All studies in this review used ICG as a fluorescence marker. The selected studies were divided into the following fields: vascular surgery (n= 18), gastrointestinal surgery (n=8), plastic surgery (n=15), neurosurgery (n=14), and

transplantation surgery (n=2). Furthermore, 1 diabetes mellitus study, 1 thyroid surgery study, and 1 study regarding the imaging of breast lesions were also included. All studies were published during the period from 2008 to 2021. An overview of the perfusion parameters mentioned in the literature is reported in Table 1.

A large selection of NIRF imaging systems were used, the most common were the SPY- Elite system (n=12), Flow 800 (n=13), and the Photodynamic eye imaging system (n=13). The reviewed articles mentioned a total of 26 perfusion parameters distilled from fluorescence-intensity curves. All of the reviewed articles selected a unique combination of the perfusion parameters mentioned in Table 1 and schematically shown in Figure 2 and 3.

NIRF-imaging was performed either pre- and post-operatively, or intraoperatively. Time- dependent parameters are described in all the included literature. Perfusion parameters are based on:

- Absolute fluorescence intensity
- Time
- Changes in intensity over time

Absolute intensity parameters

Multiple studies describe significant changes in intensity-related parameters. The maximum fluorescence intensity (Imax) is the most frequently mentioned parameter (n=29). Fluorescence intensity parameters also include ingress, egress, fluorescence intensity as a range in arbitrary units, and the fluorescence intensity at the end of the measurement period or study, as described in Table 1.

Inflow and outflow parameters

Inflow parameters could be calculated from the upslope segment of the time-intensity curve and could be correlated with tissue perfusion. These include time-specific parameters such as the Tmax, T1/2, time to peak intensity, and rise time (Figures 2 and 3). Once ICG has been intravenously administered an initial fluorescence signal can be detected (Tstart). Following detection of fluorescence intensity, the time taken to reach 50% of the maximum intensity (T1/2max) and the peak intensity (Tmax) could be calculated. Furthermore, during the upslope, the interaction between fluorescence intensity and time was also broadly explored, and includes the ingress rate, or the blood flow index, which are all ratios or rates of increase of fluorescence signal over time.

Outflow parameters are calculated to quantify the decrease in ICG intensity over time, thus providing information on vascular elimination. Time specific outflow parameters include the intrinsic transit time (ITT); the time needed for ICG to circulate from the arterial to the venous system. The downslope interaction between intensity and time was

quantified by the egress rate and IR 60, which is the intensity at 60 s after Tmax/ Fmax, for example.

Relative parameters

Relative parameters were also calculated by selecting and comparing two or more regions of interest, for example, a region with suspected ischemia being compared with another region with optimal perfusion, the reference region. The relative parameters were calculated by dividing the targeted perfusion value by the reference value.

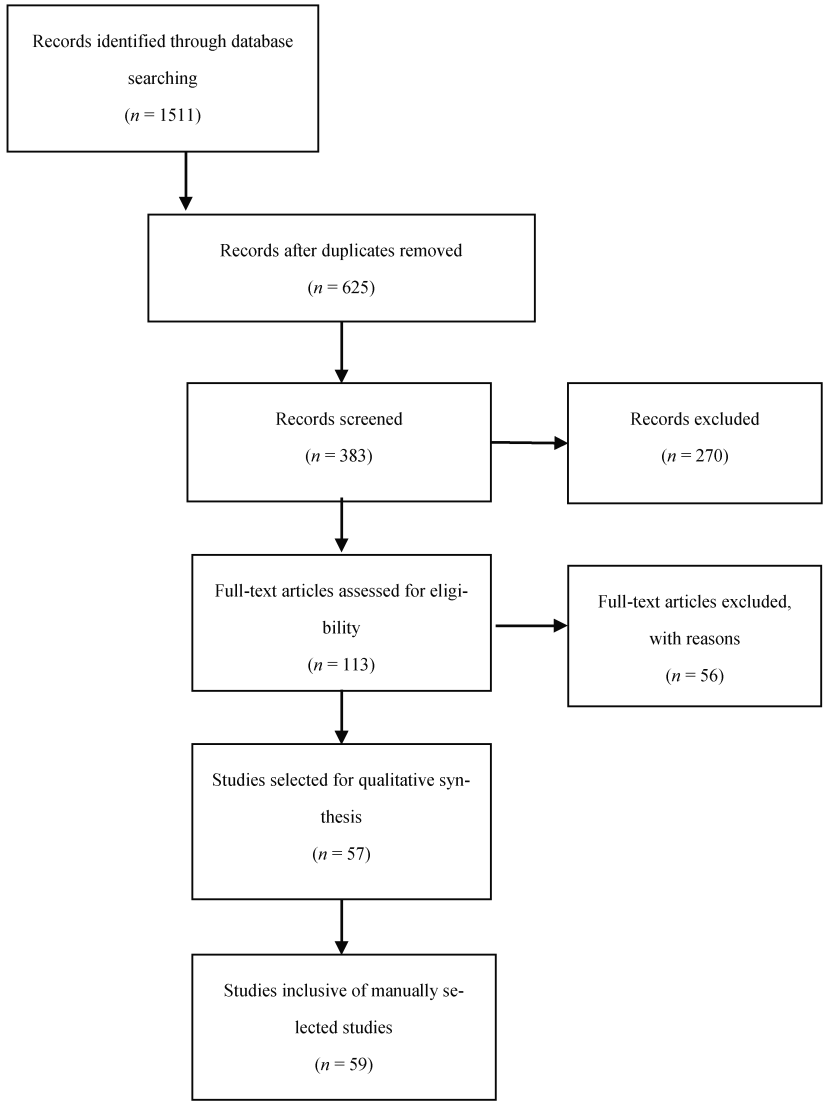

Figure 1. Preferred Reporting Items for Systematic Review and Meta-Analysis Protocols flow chart for selection of included studies.

Table 1. Overview of fluorescence perfusion parameters.

Parameter	Definition	Equivalent	References
Ingress	Absolute difference between baseline fluorescence and its maximum value		(6-17)
Ingress Rate	Rate of increase of fluorescence signal from baseline to maximum value	Wash-in rate, fluorescence signal rise, blush rate	(8-19)
Ingress AUC	Area Under the Curve from baseline to maximum fluorescence intensity	WiAUC	(19)
Egress	Absolute difference between maximum intensity and the final intensity	Washout	(6-9, 11, 14, 17, 18, 20)
Egress Rate	Rate of decrease of fluorescence signal from maximum value to the final intensity value		(8, 9, 11, 14, 17)
Fluorescence intensity	Fluorescence intensity		(8, 21-25)
Imax	Maximum fluorescence intensity	Fmax, Peak Perfusion, FImax, MFI, Cerebral blood volume	(6, 7, 24-50)
End Intensity	Fluorescence intensity at the end of the study	QEnd, residual FI	(8, 33, 51)
T start	Time to initial fluorescence signal	Tl (time local), latent time, T0, Te, TAP	(19, 28, 43, 46, 52-55)
Tmax	Time to maximum intensity	TTP (time to peak), blush time	(19, 20, 25-31, 33-43, 46, 47, 49, 53, 56, 57)
Delta T	Time from Initial fluorescent intensity to Imax	Tmax	(26, 55)
T 1/2	Time to half of the maximum fluorescence intensity	Tmax1/2, delay	(25, 27-30, 32-34, 36, 38, 39, 41, 47, 48, 58-60)
TR	Time ratio (T1/2 / Tmax)		(25)
Rise Time	Time from (10-90%) OR (20-80%) of maximum fluorescence intensity OR Time from 20-80% of maximum fluorescence intensity		(19, 33-35, 41, 45, 48, 61)
Td90%	Time from Fmax to 90% of the Fmax		(30, 39)
Td75%	Time from the Fmax to 75% of the Fmax		(30)
IR 60 sec	The rate of intensity measured 60 seconds after the Tmax to the Fmax (Intensity at 60 sec after Tmax/ Fmax)		(30)
Wash-in perfusion index	Ratio between the WiAUC to the Rise Time		(19)
Slope	Fmax/Tmax	BFI (blood flow index), Perfusion rate, Smax, Cerebral blood flow, Perfusion Index	(25, 28, 29, 34, 37, 40, 41, 43, 44, 46, 47, 49-52, 56, 57)
BFI	Blood flow Index (Fmax/RT) OR (F90-F10)/(T90-T10)	Slope	(23, 33, 35, 41, 45, 48, 58, 59, 62)
S 1/2	Slope of the intensity increase from baseline to half the maximum intensity		(37)
PDE10	The fluorescence intensity increase at 10 seconds	SPY10	(29, 37, 44, 60)
ITT	Intrinsic transit time – the time needed for the fluorescent dye to circulate from arterial to venous anastomosis	Transit time	(23, 27, 41, 45, 48, 61)
AUC	Area Under the curve of intensity over time	Curve Integral	(8)
Perfusion rate	Fraction of blood exchanged per min in vascular volume (%/min)		(20)
Relative perfusion	Perfusion as a percentage of a reference region		(6, 7, 24, 50-53, 57)

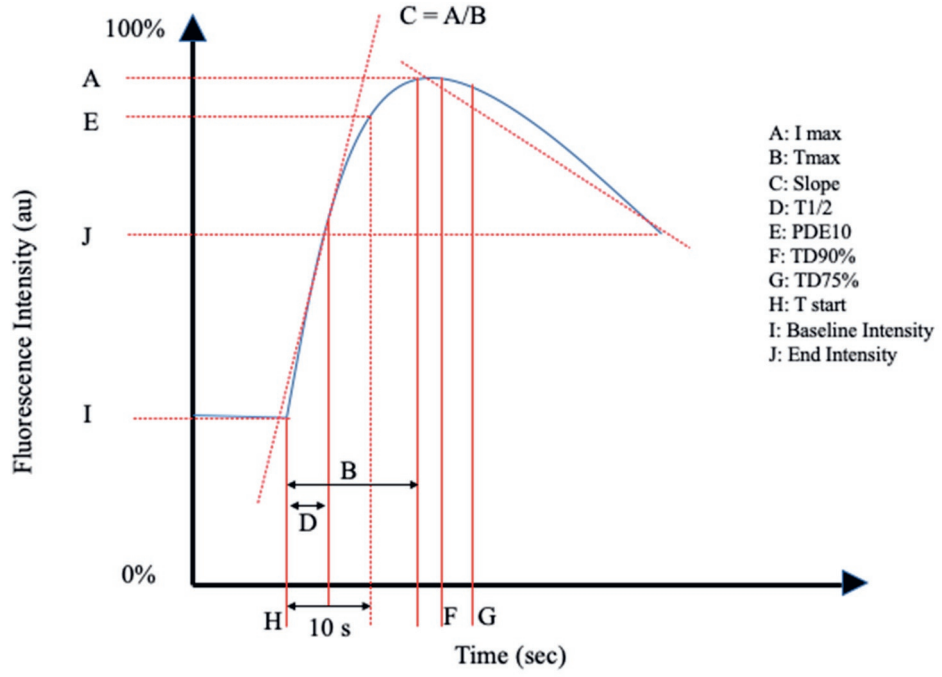

Figure 2. Schematic representation I of the perfusion parameters in Table 1.

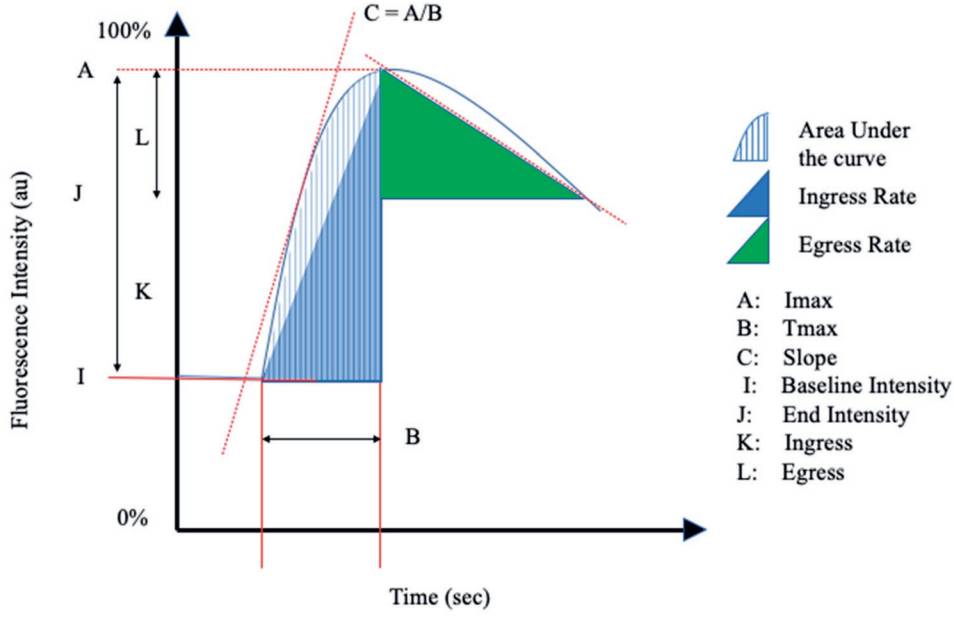

Figure 3. Schematic Representation II of the perfusion parameters in Table 1.

Gastro-intestinal Surgery

The surgical procedures discussed in this review include colorectal surgery (n=6), specifically resections followed by anastomosis, and esophagectomy (n=2). Two of the six studies on colorectal surgery performed retrospective analysis of prospective data (32, 54). Four of the eight studies on gastro-intestinal surgery included in this review administered a weight-dependent dose of ICG, as noted in Table 2 (25, 26, 54, 56).

The Fmax was researched in 6 studies (n=335) (25, 26, 28, 31, 32, 47). Four studies described no significant difference in Fmax values between groups with and without anastomotic leakage in both colorectal and oesophageal surgery (25, 26, 28, 32). Wada et al. (n=112) highlight the predictive value of Fmax for anastomotic leakage in receiver operator curve (ROC) analysis, with a sensitivity and specificity of 100% and 92% respectively at a cut-off of 52.0 units (47). The Fmax did not significantly predict early or late flatus or defecation. A study by Ishige et al. examined the application of ICG-NIRF imaging in quantifying perfusion of the gastric conduit in esophagectomy (31). A relative comparison of Fmax in a control phase, gastric tube phase, and anastomotic phase prior to intrathoracic or cervical esophago-gastronomy, was calculated and shown to be significantly different between phases, although no anastomotic leakage occurred.

Fmin was a parameter selected by Son et al. (n=86), and was described as the fluorescence intensity at the baseline (25). There was no significant difference between groups with and without anastomotic leakage.

Five studies included the Tmax as a perfusion parameter (n=245) (26, 28, 31, 47, 56). D'Urso et al. highlighted a statistically significant lengthened Tmax in both proximal and distal colorectal resection sites in the complications group in comparison to the uncomplicated cases (p=0.01) (56). Furthermore, correlation to clinical parameters such as intestinal lactate and mitochondrial efficiency showed varying significance depending on region and parameter selected (56). Amagai et al. described a significant correlation between the Tmax and anastomotic leakage in one of four selected regions of interest (p=0.015), while Hayami et al. mention no significant correlation to anastomotic leakage (26, 28). The predictive value of the Tmax in clinical outcomes such as early or late flatus or defecation is significant in 1 study (n=112) (p=0.02, p=0.01 respectively) (47). Son et al. and Amagai et al. described the Tmax as the difference between initial fluorescence intensity and maximum fluorescence intensity.(25, 26) Both studies highlighted a statistically significant difference in Tmax values between anastomotic leakage groups (Son $p<0.001$, Amagai p=0.015).

The inflow parameter T0, time to initial fluorescence signal, was studied by Aiba et al. and

Hayami et al. (28, 54). Both of the aforementioned studies showed T0 to significantly differ with regards to anastomotic leakage (Aiba p=0.046, Hayami, p=0.0022).

The TR, time ratio, is a parameter encompassing the ratio between T1/2 and Tmax and is shown to significantly differ between anastomotic leakage and no anastomotic leakage groups (n=86) (25). Furthermore, a ROC analysis with an area under the curve higher than 0.9 suggests that a TR of 0.6 is significantly predictive of anastomotic leakage (25).

T1/2 was adopted as an inflow parameter by 4 studies (n=246) (25, 28, 32, 47). Two studies by Kamiya et al. and Son et al. described a statistically significant difference in T1/2 in anastomotic failure or leakage groups ($p<0.01$, $p<0.001$ respectively) (25, 32). One study showed no significant difference between groups with and without anastomotic leakage (28).

The slope was investigated in two studies (n=134) (28, 47). No significant intraoperative difference or prediction of postoperative outcomes was described.

Neurosurgery

Fourteen studies (n=345) investigated the application of ICG angiography in vascular neurosurgery (27, 33-35, 41, 45, 48, 49, 58, 59, 61-64). Eight of the fourteen studies selected for dose-dependent ICG administration, with doses ranging from 0.1mg/kg to 0.3mg/kg, see Table 2 for further details. The studies analyzed the following inflow parameters: Tmax, T1/2, RT, slope, transit time and cerebral blood flow index. The rise time is heterogeneously defined as the interval between 10% and 90% of the signal, or 20% and 80% of the signal.

The Tmax parameter was examined in seven studies (n= 191) (27, 33-35, 41, 49, 63). One study found the Tmax to significantly discriminate between patients with impaired and normal cerebral perfusion in occlusive cerebral arterial disease and control groups (p=0.013).(35) Furthermore, the ratio of Tmax pre- and post-bypass procedure was significantly lower in patients with postoperative hyperperfusion syndrome than in patients without postoperative hyperperfusion syndrome (p=0.017) (35).

The T1/2 was explored in four articles (n=181) (27, 48, 58, 59). Three studies researched the application of this perfusion parameter in patients pre- and post-bypass surgery, with only one study by Prinz et al. reporting a significant decrease (p=0.001) (27, 58, 59). However, when Prinz et al. compared the ICG perfusion data to quantitative Doppler flow, there were no significant correlations between the diagnostic methods.

Four articles (n=44) selected rise time (RT) as an ICG perfusion parameter (33, 35, 45, 61). Holling et al. found RT to be significantly shorter following a bypass procedure (p=0.025), with no change between pre- and post-bypass data in control measurements (p=0.125) (61). A study by Kamp et al. exploring cortical perfusion following traumatic brain injury found the arterial RT to be significantly longer in in patients with a favourable outcome at 3 months (p=0.002).

Of the four studies (n=153) that calculated transit time as a perfusion parameter, two studies by Holling et al. and Ye et al described significant results (27, 41, 48, 61). Ye et al. highlighted a significant difference in arteriovenous transit time in a heterogenous group of patients including arteriovenous malformations, Moyamoya disease and both unruptured and ruptured cerebral aneurysms (48).

Cerebral blood flow (CBF), or slope, was the most commonly selected neurovascular perfusion parameter, mentioned in ten articles (n=246) (35, 41, 58, 63, 64). 7 studies examined the change in cerebral blood flow pre- and post-bypass procedure (35, 41, 49, 58, 59, 63, 64). A statistically significant change in CBF was noted in five of the aforementioned seven studies (35, 41, 58, 63, 64). Four studies also examined the relationship between the development of postoperative hyperperfusion and CBF, with two studies by Zhang et al. and Uchino et al. describing a significant increase in CBF in the symptomatic hyperperfusion group ($p<0.001$, $p=0.013$ respectively) (35, 49, 63, 64).

One study by Kamp et al. describes the parameter residual fluorescence intensity, as a percentage of maximum fluorescence intensity, in patients with traumatic brain injury (33). The cortical and venous residual fluorescence intensity was significantly higher in cortical and venous tissue ($p=0.01$, $p=0.02$ respectively) in patients with an unfavourable outcome. No significant difference was noted in arterial residual fluorescence intensity ($p=0.05$).

Absolute fluorescence intensities were calculated in nine studies (27, 33-35, 41, 45, 48, 49, 63). Five studies found a significantly different Imax value between perfusion groups (35, 45, 48, 49, 63). Kobayashi et al. noted a significant increase in Imax after STA-MCA bypass surgery ($p=0.047$), yet no significant difference in Imax values when comparing patients with and without postoperative hyperperfusion (35). However, Zhang et al. also investigated Imax as a perfusion parameter in the detection of postoperative hyperperfusion and described a significantly higher Imax in the symptomatic hyperperfusion group ($p<0.001$) (49).

Plastic Surgery

Fluorescent imaging was quantitatively reported in fifteen articles, including 515 patients (6, 7, 10, 13, 17, 19, 22, 23, 36, 37, 46, 51-53, 57). The fields of application include free-flap and DIEP flap perfusion, breast reconstruction surgery, and microvascular surgery. The SPY Elite Imaging system was most commonly selected (n= 8), see Table 2.

Flap perfusion

Flap perfusion studies examined free flap surgery, flap perfusion in maxillofacial surgery, and DIEP flap procedures. Relative perfusion was researched in three studies (6, 7, 52). Abdelwahab et al. showed the flap-to-cheek ratio to be statistically significant in predicting flap vascularisation, while Betz et al. highlight no significant difference in relative slope values in free flap surgery (6, 7, 52).

Inflow and outflow parameters were mentioned in seven (n=128) free-flap and DIEP flap studies (10, 13, 23, 36, 37, 52, 53). Two studies described no significant differences in the ingress and ingress rate (10, 13). Significant differences in inflow parameters including the slope, Tmax, PDE10, slope at T1/2, and T1/2 were seen in three studies (23, 37, 53). Hitier et al. described a significantly lower per-operative Fmax in flaps with vascular complications (p=0.008) (23). Furthermore, in flaps with a significantly lower postoperative slope (p=0.02) and Fmax (p=0.03) values returned to normal following surgical revision (23). One study examining single-pedicle versus bipedicle blood supply in flap reconstruction found no significant difference in the Imax between the aforementioned groups, with a significant difference in the Tmax, T1/2, slope, PDE10, and slope at T1/2 between the same groups ($p<0.05$) (37).Absolute intensity parameters were not significant in studies by Betz et al. and Miyazaki et al. (37, 53).

Breast Reconstructive surgery

Gorai et al. explored the use of relative ICG perfusion parameters in the prediction of skin necrosis following tissue expander reconstruction in breast cancer patients (57). The application of ICG imaging lead to a significant lower rate of necrosis ($p<0.05$), with a statistically significant difference in relative perfusion ($p<0.001$). Yang et al. evaluated mastectomy flap perfusion at various tissue expander volumes, with significant differences in the ingress and egress between different expander volume groups (p=0.0001, p=0.0037 respectively) (17).

Microvascular Surgery

Reconstructive surgical procedures are dependent on adequate vascular and nervous supply to the operated region. Tanaka et al. explored the use of ICG imaging to detect blood supply to the femoral cutaneous- and vastus lateralis motor nerve, allowing for the

selection of the better vascularised nerve (46). The selected inflow parameters slope and Tstart, were heterogenous statistically significant, while the Tmax showed no statistical significance in any region measured (46). Fichter et al. examined the effect of the number of osteotomies on bone perfusion in free fibula flaps (19). The study found a significant differences in the slope with additional osteotomies ($p=0.034$). Mothes et al. explored tissue perfusion during hand revascularisation surgery, and found intraoperative slope values to significantly differ in tissue that survived postoperatively ($p<0.01$) (51). Three studies (n=75) researched absolute fluorescent intensity, namely the Imax, reporting heterogenous results depending on time points or regions selected for comparison (22, 46, 51).

Vascular Surgery

Quantitative analysis of fluorescence imaging was conducted in 18 studies included in this review (n=683) (8, 11, 12, 15, 16, 18, 20, 29, 30, 38-40, 43, 44, 50, 55, 60, 65). Fifteen studies opted for dose-dependent ICG administration, with 10 studies selecting a dose of 0.1mg/kg (8, 11, 12, 15, 16, 18, 20, 29, 30, 38-40, 43, 44, 50, 55, 60, 65). SPY Elite Imaging was the fluorescence imaging system of choice in eight studies, see Table 2. The fields of application within vascular surgery include patients with PAD, patients receiving dialysis, prediction of wound healing, microperfusion following arteriovenous fistula formation in dialysis patients, and perfusion in Raynaud's phenomenon.

The Fmax was the most frequently selected parameter (7 studies; n=297) (18, 29, 30, 38-40, 50). Four studies described a significant difference in the Fmax pre- and post-revascularisation, with Nakamura et al. mentioning no significant difference in the treated limb and a significant decrease in the contralateral limb ($p=0.0875$, $p=0.006$ respectively) (18, 29, 38, 40). No significant difference in Fmax was detected between PAD patients and controls; dialysis patients and controls, Rutherford Classification categories; or critical limb ischemia patients and controls (30, 39, 50).

Six studies selected the ingress and ingress rate as a perfusion parameter (n=237) (8, 12, 15, 16, 18, 40). Five studies evaluated the Ingress in PAD patients, all describing statistically significant results pre- and post-revascularisation (8, 15, 16, 18, 40). Regus et al. highlighted a statistically significant difference in the Ingress and Ingress rate pre- and post-arteriovenous anastomotic creation in the hand and fingers of dialysis patients ($p<0.001$) (12). Furthermore, there was a significant difference in the intraoperative Ingress ratio and Ingress rate ratio in patients who developed hemodialysis access-induced distal ischemia ($p=0.001$, $p=0.003$ respectively) (12).

The egress and egress rate provided heterogenous results in PAD patients undergoing revascularisation procedures in two studies (8, 18). One study by Braun et al shows a significant difference in both the Egress and Egress rate pre- and post-revascularisation ($p=0.004$, $p=0.013$ respectively), while there is no significant difference in the Egress in a study by Colvard et al. ($p=0.35$) (8, 18).

The perfusion parameter Tmax was discussed in six studies (n=204) (29, 30, 38, 39, 55). Heterogenous results were seen in PAD patients pre- and post-revascularisation. Igari et al. described a significant difference in the Tmax in 3 regions of interest following revascularisation (29). A study by Nakamura et al. also found the Tmax to be significantly different post-revascularisation, in both the intervention limb and the contralateral limb ($p=0.016$, $p=0.013$ respectively) (38). Only one study examined the Tmax in PAD and control patients, with a significant difference between the groups ($p<0.05$) (30).

Six studies selected the T1/2 as a perfusion parameter (29, 30, 38, 39, 60, 65). One study by Venermo et al. showed no significant different in T1/2 between patients with and without diabetes (65). Igari et al. state no significant difference between PAD patients and controls (30). Two studies describe significant changes in the T1/2 in PAD patients pre- and post-revascularisation (29, 38).

Studies exploring the T1/2 in patients with diabetes, on dialysis and grouped according to Fontaine Classification or critical limb ischemia showed heterogenous results (39, 60, 65).

Two studies (n=51) examined the slope (29, 50). One study showed a significant change in the slope in three selected regions of interest following revascularisation in PAD patients (n=21) (29). A study by Zimmermann et al. described a significant difference in the slope in patients grouped according to the Rutherford classification; with increased extent of arterial collateralisation; and in patients with critical limb ischemia ($p<0.001$, $p=0.005$, $p<0.001$) (50).

The PDE10, described as the fluorescence intensity increase at 10 seconds, was examined in four studies (29, 44, 60, 65). Two studies state a statistically significant change in the PDE10 in PAD patients following a revascularisation procedure (29, 44). An ROC analysis was performed in two studies, with a cut-off PDE10 of 28 s at a transcutaneous pressure (TcPO2) of 30mmHg in a study by Terasaki et al., and a cut-off PDE10 of 21 arbitrary units at a TcPO2 of 40mmHg in a study by Venermo et al. (60, 65).

Eleven of the eighteen vascular surgery studies included in this review assessed the correlation between the aforementioned perfusion parameters and standard diagnostic

methods in this field such as the ankle-brachial index (ABI), toe pressure, TcPO2 and the toe brachial index (TBI) (8, 11, 18, 29, 30, 38, 40, 43, 44, 50, 65). Four studies found no significant correlation between ABI and ICG-NIRF perfusion parameters (11, 38, 40, 44). Significant but heterogenous correlation is seen between the ABI and a range of parameters in five studies (8, 18, 29, 30, 65).

Transplantation

Two studies (n=205) explored the application of quantitative ICG imaging in transplantation surgery (9, 14). Both studies utilised the SPY Elite Imaging System and an ICG dose of 0.02mg/kg. Inflow parameters ingress, ingress rate, egress and egress rate were assessed. Rother et al. and Gerken et al. describe the ingress and ingress rate to significantly detect differences in kidney perfusion. Gerken et al. explores the association of intraoperative ICG angiography with delayed graft function, describing a cut off ingress value of 106.23AU for the prediction of delayed graft function with a sensitivity of 78.3% and specificity of 80.8% ($p<0.0001$) (9). No further mention of data related to the egress or egress rate are noted by Rother et al. (14).

Other

Diabetic Wound healing

Hajhosseini et al. researched the application of ICG angiography in the prediction of diabetic wound healing following hyperbaric oxygen therapy in cases and controls (21). Absolute fluorescence intensity was selected as perfusion parameter, showing a significant improvement between pre- and post-hyperbaric oxygen therapy in the patient group ($p<0.0015$).

Total thyroidectomy

Parathyroid function and perfusion was intraoperatively measured by ICG angiography, assessing if the diagnostic could predict postoperative hypocalcaemia (24). Relative perfusion parameters based on absolute fluorescent intensity and average fluorescence intensity were selected, with the anterior trachea as reference region. Relative absolute fluorescence intensity was predictive of both postoperative hypocalcaemia ($p=0.027$), and a postoperative drop in parathyroid hormone ($p<0.001$). Relative average fluorescence intensity provided no significant results.

Breast imaging

Schneider et al evaluated ICG imaging in the detection and characterisation of breast

lesions, namely malignant and benign (42). Inflow parameters peak amplitude (Imax) and time to peak (Tmax) were selected. A peak time-grouped amplitude was calculated, an average of amplitudes in malignant and benign lesions at 30 time-points. A significant difference in peak amplitude was noted between the two groups (p=0.00015).

Table 2. Overview of study characteristics and results of near-infrared fluorescence imaging.

Application	Reference	Study Characteristics			
		Patients	***Camera***	***Software***	***ICG dose***
Gastro-intestinal Surgery	Aiba(54)	110	OPAL1	Not spec	0.1mg/kg
	Amagai(26)	69	Karl Storz	ImageJ	0.2mg/kg
	D'Urso(56)	22	D-Light P	FLER	0.2mg/kg
	Hayami(28)	22	D-Light P	Hamamatsu Photonics	5mg/2ml
	Ishige(31)	20	Olympus	Hamamatsu Photonics	1.25mg
	Kamiya(32)	26	PDE Hamamatsu	Hamamatsu Photonics	1ml
	Son(25)	86	Image1	Tracker 4.97	0.25mg.kg
	Wada(47)	112	PDE Hamamatsu	Hamamatsu Photonics	5mg
Neurosurgery	Goertz(27)	54	Carl Zeiss Co.	Flow 800	10mg
	Holling(61)	5	OPMI Pentero Microscope	Flow 800	5mg
	Kamp(33)	10	OPMI Pentero Microscope	Flow 800	5mg
	Kamp(34)	30	OPMI Pentero Microscope	Flow 800	5mg
	Kobayashi(35)	10	OPMI Pentero Microscope	Flow 800	7.5mg/3ml
	Prinz(58)	30	OPMI Pentero Microscope	Flow 800	0.25mg/kg
	Rennert(41)	7	OPMI Pentero Microscope	Flow 800	0.2mg/kg
	Rennert(59)	10	OPMI Pentero Microscope Or Kinevo	Flow 800	0.2mg/kg
	Shi(45)	9	OPMI Pentero Microscope	Flow 800	0.1mg/kg
	Uchino(64)	10	OPMI Pentero Microscope	Flow 800	0.1mg/kg
	Uchino(63)	7	OPMI Pentero Microscope	Flow 800	0.1mg/kg
	Woitzik(62)	6	IC-View	IC Calc	0.3mg/kg
	Ye(48)	87	Carl Zeiss Co.	Flow 800	0.25mg/kg
	Zhang(49)	60	Not spec	Flow 800	Not spec
Plastic Surgery	Abdelwahab(6)	71	SPY Elite Imaging System	SPY-Q	5mg/2ml
	Abdelwahab(7)	10	SPY Elite Imaging System	SPY-Q	5mg/2ml
	Betz(52)	11	Karl Storz	IC Calc	0.3mg/kg
	Betz(53)	25	ICG Pulsion	IC Calc	0.3mg/kg
	Fichter(19)	40	Pulsion PDE	ImageJ	0.3mg/kg
	Girard(10)	40	SPY Elite Imaging System	SPY-Q	5mg
	Gorai(57)	181	PDE Hamamatsu	Hamamatsu Photonics	25mg/2ml
	Han(22)	32	SPY Elite Imaging System	Not spec	2.5mg
	Hitier(23)	20	Fluobeam	Fluobeam	0.25mg/kg
	Maxwell(36)	1	SPY Elite Imaging System	Not spec	Not spec
	Miyazaki(37)	8	PDE Hamamatsu	Hamamatsu Photonics	0.1mg.kg
	Mothes(51)	35	IC-View	IC Calc	0.5mg/kg
	Rother(13)	23	SPY Elite Imaging System	SPY-Q	0.1mg/kg
	Tanaka(46)	8	PDE Hamamatsu	Hamamatsu Photonics	0.1mg/kg

	Yang(17)	10	SPY Elite Imaging System	SPY-Q	3ml
Vascular	Braun(8)	24	SPY Elite Imaging System	Not spec	Not spec
	Colvard(18)	93	SPY Elite Imaging System	SPY-Q	2.5ml
	Igari(29)	21	PDE Hamamtsu	Hamamatsu Photonics	0.1mg/kg
	Igari(30)	23	PDE Hamamtsu	Hamamatsu Photonics	0.1mg/kg
	Kang(55)	2	Vieworks	Visual C++	0.16mg/kg
	Kang(20)	2	VIeworks	Not spec	0.16mg/kg
	Mironov(11)	28	SPY Elite Imaging System	SPY-Q	5mg/250ml
	Nakamura(38)	21	PDE Hamamatsu	Hamamatsu Photonics	0.1mg/kg
	Nishizawa(39)	62	PDE Hamamatsu	Hamamatsu Photonics	0.1mg/kg
	Patel(40)	47	SPY Elite Imaging System	Not spec	0.1mg/kg
	Regus(12)	47	SPY Elite Imaging System	SPY-Q	0.002mg/kg
	Rother(15)	40	SPY Elite Imaging System	SPY-Q	0.1mg/kg
	Rother(16)	33	SPY Elite Imaging System	SPY-Q	0.1mg/kg
	Seinturier(43)	34	Fluobeam	Not spec	0.05mg/kg
	Settembre(44)	101	SPY Elite Imaging System	Not spec	0.1mg/kg
	Terasaki(60)	34	PDE Hamamatsu	Hamamatsu Photonics	0.1mg/kg
	Venermo(65)	41	PDE Hamamatsu	Hamamatsu Photonics	0.1mg/kg
	Zimmermann(50)	30	IC-View	IC-Calc	0.5mg/kg
Transplantation	Rother(14)	77	SPY Elite Imaging System	SPY-Q	0.02mg/kg
	Gerken(9)	128	SPY Elite Imaging System	SPY-Q	0.02mg/kg
Thyroid Surgery	Lang(24)	70	SPY Elite Imaging System	Not spec	2.5mg
Diabetic Foot	Hajhosseini(21)	21	LUNA Fluorescence Microscope	SAS	5mg/ml
Breast lesions	Schneider(42)	30	NIRx Medical Technologies	NIRx NAVI	2.5mg

Discussion

This review highlights the broad selection of perfusion parameters in NIRF imaging. NIRF-imaging shows great potential as a surgical tool with applications in gastro-intestinal, plastic, vascular and neurosurgery. However, the quantification of NIRF-imaging and selection of optimal perfusion parameters faces several challenges. The studies included in this review were largely performed in a small cohort setting, randomised clinical studies have yet to be performed. Research in this field to date is heterogeneous in study design, methodology, selected perfusion parameters and endpoints. The heterogeneity in perfusion parameters selected and the large variation in significance of outcomes in the articles presented in this review highlight the need for procedure-specific parameters and protocols to allow for clinical application of this technique. Before the application of quantitative perfusion analysis in a clinical setting, comparison of perfusion parameters in cases and controls is advised for baseline values. While intensity dependent parameters are frequently discussed, they are susceptible to

intra- and interpatient variability. Intensity dependent parameters can vary with changes in the imaging setting such as light intensity or camera angulation or distance from the patient. Statistical significance is often in a relative pre- and post-intervention setting, with no correlation to standard perfusion techniques such as the ankle–brachial index. Time-related parameters such as the Tmax or T1/2max are commonly mentioned as the parameters of choice, due to a reduced influence of fluorescence intensity as mentioned above. Furthermore, time-related parameters allow for the selection and measurement of regions of interest (ROIs) with a different camera distance and angle. This is advantageous in gastrointestinal surgery for example, where perfusion pre- and post-anastomosis needs to be documented.

Relative perfusion parameters are a favourable option for a clinical setting, to a degree removing the influence of fluorescence intensity. Problems occur in a setting where the perfusion in the reference region is incorrectly assumed to be sufficient or is difficult to calculate. Peripheral arterial disease patients illustrate the pitfalls in relative parameters, with the example of a patient set to undergo an above the knee amputation. A large majority of patients also have arterial disease in the contralateral limb raising making the reference perfusion value less reliable. Furthermore, should the patient already have a below the knee amputation of the intervention limb, it would not be feasible to film comparable sections of limb with one ICG dose. Table 3 summarizes the advantages and disadvantages of the various methods of quantification in NIRF imaging. Limitations in this field concern the fluorescence angiography technique. In vascular surgery, the presence of inflammation or necrosis can impact the fluorescence signal. Inflammation leads to vasodilatation and hyperemia, falsely increasing the intensity-related parameters (43). The influence of reactive hyperperfusion following a revascularization procedure in the field of vascular surgery also requires further research, as it remains unclear if post-revascularization NIRF measurements are representative of the patient's vascular status. The influence of the circulatory status of the patient on NIRF parameters, such as Tmax or T1/2, is unclear. Theoretically, hypotension or reduced cardiac output could explain a lengthened Tmax, rather than the presence of an occlusion in neurovascular or vascular surgery. Furthermore, the impact of a patient's plasma protein level on ICG uptake, and the subsequent intensity of the ICG measured requires further research. The validity of quantified fluorescence data is further distorted by the range in ICG dose, camera selection, camera and environmental settings and quantification software. Imaging systems have different sensitivities to fluorescence signals, creating heterogenous data before factoring in the impact of environmental influences. Son et al selected an Image1 S fluorescence imaging system and (Tracker 4.97, Douglas Brown, Open Source Physics, Boston MA, USA) quantification software, while Wada et al chose a PDE-neo system and ROIs (Hamamatsu Photonics K.K.) analysis software (25, 47). The abovementioned differences between studies are explored in a recent systematic review

by Lutken et al. (66). The authors describe the diversity in perfusion parameters and methodology in the field of gastro-intestinal surgery, concluding that the application of ICG-NIRF imaging in this field requires standardisation before implementation in a clinical setting. A potential means of achieving standardization is by the process of normalization, a mathematical means of correcting for fluctuations in fluorescence intensity, as yet only described in animal studies with promising results (67-69).

Table 3. Summary of methods of quantification in NIRF imaging.

Parameter	Advantages	Disadvantages
Intensity-related parameters	Broad parameter selection	Influencing factors on intensity: - Patient-related: ICG concentration, cardiac output - System-related: camera distance, camera angle, environmental light
Time-related parameters	No influence of measured intensity Comparison possible between ROIs with different camera distance and angle	Narrow parameter selection
Relative parameters	Patient vasculature provides case-control data	Reference region may not be representative of optimal perfusion Influencing factors on intensity (see above)

Conclusion

In conclusion, quantitative analysis of fluorescence imaging has made great advances in recent years, showing potential across multiple surgical fields both intraoperatively, and in the relative pre- and postoperative evaluation of an intervention. Considering the rapidly growing application of this technique, research of the underlying quantification process is deficient. In this review we have explored the perfusion parameters currently used in various surgical specializations. While this review highlights the heterogenicity in parameter selection, time-related parameters appear superior to absolute fluorescence intensity parameters in quantifying perfusion. Before ICG-NIRF imaging can be considered as the as a gold standard of perfusion quantification, standardisation of parameter selection, and methodology with regard to ICG dose and camera type need to be explored.

Appendices

Appendix A. Search strategy.

Pubmed

("Perfusion"[Mesh] OR "perfus*"[tw] OR "reperfus*"[tw]) AND ("Indocyanine green"[Mesh] OR "indocyanin*"[tw] OR "ICG"[tiab] OR "Wofaverdin*"[tw] OR "Vophaverdin*"[tw] OR "Vofaverdin*"[tw] OR "Cardio-Green*"[tw] OR "Cardio Green*"[tw] OR "Cardiogreen*"[tw]) AND ("paramet*"[tw] OR "variable"[tw] OR "variables"[tw]) OR (("Perfusion"[majr] OR "perfus*"[ti] OR "reperfus*"[ti]) AND ("Indocyanine green"[Majr] OR "indocyanin*"[ti] OR "ICG"[ti] OR "Wofaverdin*"[ti] OR "Vophaverdin*"[ti] OR "Vofaverdin*"[ti] OR "Cardio-Green*"[ti] OR "Cardio Green*"[ti] OR "Cardiogreen*"[ti] OR ("cardio"[ti] AND "green"[ti]))

Medline

(exp Perfusion/ OR "perfus*".mp. OR "reperfus*".mp.) AND (exp Indocyanine green/ OR "indocyanin*".mp. OR "ICG".ti,ab. OR "Wofaverdin*".mp. OR "Vophaverdin*".mp. OR "Vofaverdin*".mp. OR "Cardio-Green*".mp. OR "Cardio Green*".mp. OR "Cardiogreen*".mp.) AND ("paramet*".mp. OR "variable".mp. OR "variables".mp.) OR ((*exp Perfusion/ OR "perfus*".ti. OR "reperfus*".ti.) AND (exp *Indocyanine green/ OR "indocyanin*".ti. OR "ICG".ti. OR "Wofaverdin*".ti. OR "Vophaverdin*".ti. OR "Vofaverdin*".ti. OR "Cardio-Green*".ti. OR "Cardio Green*".ti. OR "Cardiogreen*".ti. OR ("cardio".ti. AND "green".ti.)))

Embase

(exp Perfusion/ OR "perfus*".mp. OR "reperfus*".mp.) AND (exp Indocyanine green/ OR "indocyanin*".mp. OR "ICG".ti,ab. OR "Wofaverdin*".mp. OR "Vophaverdin*".mp. OR "Vofaverdin*".mp. OR "Cardio-Green*".mp. OR "Cardio Green*".mp. OR "Cardiogreen*".mp.) AND ("paramet*".mp. OR "variable".mp. OR "variables".mp.) OR ((*exp Perfusion/ OR "perfus*".ti. OR "reperfus*".ti.) AND (exp *Indocyanine green/ OR "indocyanin*".ti. OR "ICG".ti. OR "Wofaverdin*".ti. OR "Vophaverdin*".ti. OR "Vofaverdin*".ti. OR "Cardio-Green*".ti. OR "Cardio Green*".ti. OR "Cardiogreen*".ti. OR ("cardio".ti. AND "green".ti.)))

Cochrane

(("perfus*" OR "reperfus*") AND ("indocyanin*" OR "ICG" OR "Wofaverdin*" OR "Vophaverdin*" OR "Vofaverdin*" OR "Cardio-Green*" OR "Cardio Green*" OR "Cardiogreen*" OR ("cardio" AND "green")))

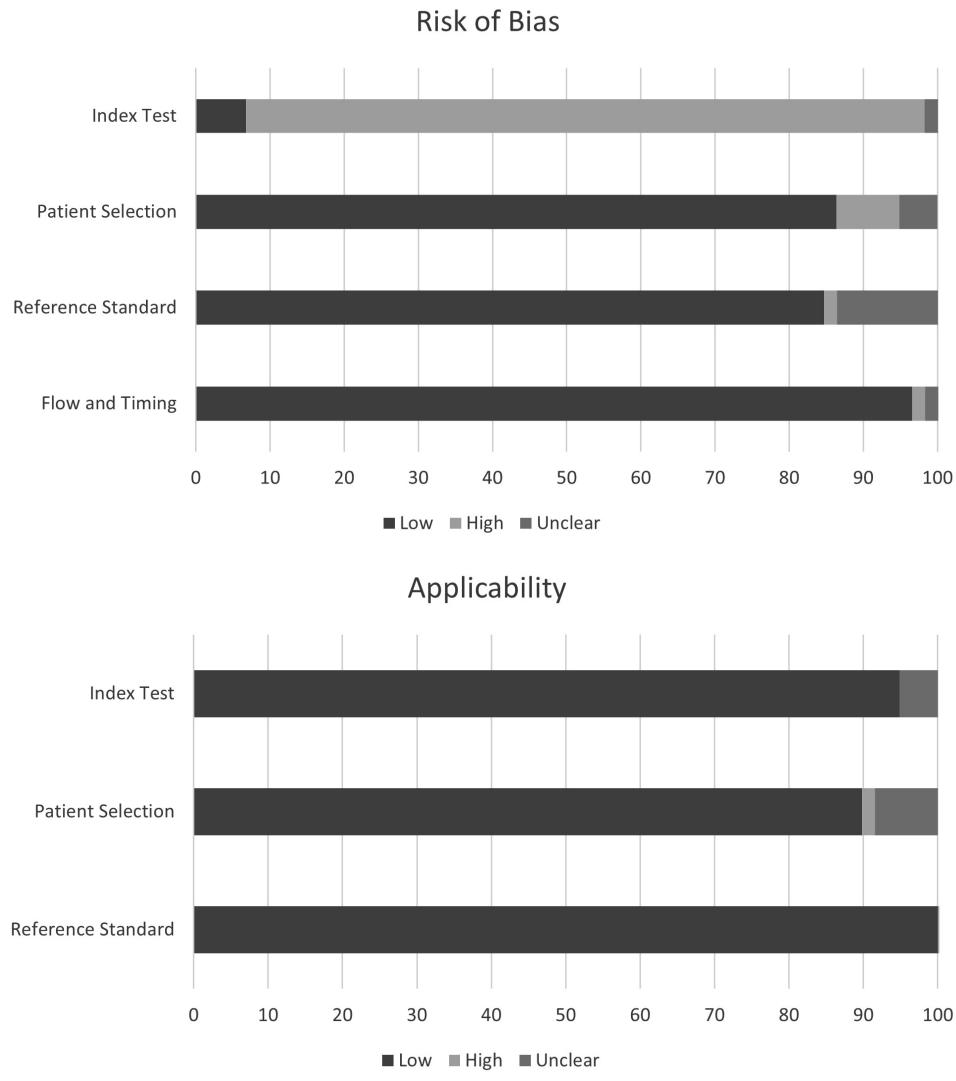

Figure S1. Proportion of studies with low, high, and unclear risk of bias according to the revised Quality Assessment of Diagnostic Accuracy Studies.

Table S1. Quality assessment and risk of bias according to the revised Quality Assessment of Diagnostic Accuracy Studies.

	Applicability Concerns				Risk of bias		
Study	**Patient Selection**	**Index test**	**Reference Standard**	**Flow and Timing**	**Patient Selection**	**Index test**	**Reference Standard**
Abdelwahab, 2019(6)	-	+	?	-	-	-	-
Abdelwahab, 2019(7)	+	+	?	-	-	-	-
Aiba, 2021(54)	-	+	?	-	-	-	-
Amagai, 2020(26)	-	+	-	-	-	-	-
Betz, 2009(52)	-	+	-	-	-	-	-
Betz, 2013(53)	-	+	-	-	-	-	-
Braun, 2013(8)	-	+	-	-	-	-	-
Colvard, 2016(18)	-	+	-	-	-	-	-
D'urso, 2020(56)	-	+	-	-	-	-	-
Fichter, 2019(19)	-	+	?	-	-	-	-
Gerken, 2020(9)	-	+	-	-	-	-	-
Girard, 2019(10)	-	+	-	-	-	-	-
Goertz, 2019(27)	-	+	?	-	-	-	-
Gorai, 2017(57)	-	+	-	-	-	-	-
Hajhosseini, 2021(21)	-	+	?	+	-	-	-
Han, 2018(22)	-	+	-	-	-	-	-
Hayami, 2019(28)	-	+	-	-	-	-	-
Hitier, 2016(23)	-	+	-	-	-	-	-
Holling, 2013(61)	-	+	-	-	-	-	-
Igari, 2013(29)	-	+	-	-	-	-	-
Igari, 2014(30)	+	+	-	-	+	-	-
Ishige, 2019(31)	-	+	?	-	-	?	-
Kamiya, 2015(32)	-	+	-	-	-	-	-
Kamp, 2017(33)	-	+	-	-	-	-	-
Kamp, 2012(34)	-	?	-	-	-	?	-
Kang, 2011(55)	+	+	-	-	?	-	-
Kang 2010(20)	+	+	-	-	?	-	-
Kobayashi, 2014(35)	-	+	-	-	-	-	-
Lang, 2017(24)	-	+	-	-	-	-	-
Maxwell, 2016(36)	+	+	-	-	?	-	-
Mironov, 2019(11)	-	-	-	-	-	-	-
Miyazaki, 2017(37)	-	+	-	-	-	-	-

Mothes, 2009(51)	-	+	-	-	-	-	-
Nakamura, 2017(38)	-	+	-	-	-	-	-
Nishizawa, 2017(39)	-	+	-	-	-	-	-
Patel, 2018(40)	-	+	-	-	-	-	-
Prinz, 2014(58)	-	+	?	-	-	-	-
Regus, 2019(12)	-	+	-	-	-	-	-
Rennert, 2018(41)	-	+	-	-	-	-	-
Rennert, 2019(59)	-	+	-	-	-	-	-
Rother, 2019(14)	-	+	-	-	-	-	-
Rother, 2018(15)	-	+	-	-	-	-	-
Rother, 2017(16)	-	+	-	-	-	-	-
Rother, 2020(13)	?	+	-	-	-	-	-
Schneider, 2011(42)	?	+	-	-	?	-	-
Seinturier, 2020(43)	-	+	-	?	-	-	-
Settembre, 2017(44)	-	+	-	-	-	-	-
Shi, 2015(45)	-	+	-	-	-	-	-
Son, 2019(25)	-	+	-	-	-	-	-
Tanaka, 2015(46)	-	+	-	-	-	-	-
Terasaki, 2013(60)	-	+	-	-	-	-	-
Uchino, 2014(64)	-	+	-	-	-	-	-
Uchino, 2013(63)	-	+	-	-	-	-	-
Venermo, 2016(65)	-	+	-	-	-	-	-
Wada, 2017(47)	-	-	-	-	-	-	-
Woitzik, 2006(62)	?	+	?	-	?	?	-
Yang, 2018(17)	-	+	-	-	-	-	-
Ye, 2013(48)	-	+	-	-	-	-	-
Zhang, 2020(49)	-	+	-	-	-	-	-
Zimmermann, 2012(50)	-	+	-	-	-	-	-

-, Low risk of bias; + high risk of bias; ? risk of bias unclear

Reference List

1. Cornelissen AJM, van Mulken TJM, Graupner C, Qiu SS, Keuter XHA, van der Hulst RRWJ, et al. Near-infrared fluorescence image-guidance in plastic surgery: A systematic review. Eur J Plast Surg. 2018;41(3):269-78.
2. al PvdHe. A systematic review of the use of near-infrared fluorescence imaging in patients with peripheral artery disease. Journal of Vascular Surgery. 2019;70(1).
3. Singh SKMDM, Desai NDMDP, Chikazawa GMDP, Tsuneyoshi HMDP, Vincent JB, Zagorski BMM, et al. The Graft Imaging to Improve Patency (GRIIP) clinical trial results. J Thorac Cardiovasc Surg. 2010;139(2):294-301.e1.
4. Mangano A, Masrur MA, Bustos R, Chen LL, Fernandes E, Giulianotti PC. Near-Infrared Indocyanine Green-Enhanced Fluorescence and Minimally Invasive Colorectal Surgery: Review of the Literature. Surg Technol Int. 2018;33:77-83.
5. Whiting PF, Rutjes AWS, Westwood ME, Mallett S, Deeks JJ, Reitsma JB, et al. QUADAS-2: a revised tool for the quality assessment of diagnostic accuracy studies. Ann Intern Med. 2011;155(8):529-36.
6. Abdelwahab M, Kandathil CK, Most SP, Spataro EA. Utility of Indocyanine Green Angiography to Identify Clinical Factors Associated With Perfusion of Paramedian Forehead Flaps During Nasal Reconstruction Surgery. JAMA Facial Plast Surg. 2019;21(3):206-12.
7. Abdelwahab M, Spataro EA, Kandathil CK, Most SP. Neovascularization Perfusion of Melolabial Flaps Using Intraoperative Indocyanine Green Angiography. JAMA Facial Plast Surg. 2019;21(3):230-6.
8. Braun JD, Trinidad-Hernandez M, Perry D, Armstrong DG, Mills JL, Sr. Early quantitative evaluation of indocyanine green angiography in patients with critical limb ischemia. J Vasc Surg. 2013;57(5):1213-8.
9. Gerken ALH, Nowak K, Meyer A, Weiss C, Kruger B, Nawroth N, et al. Quantitative Assessment of Intraoperative Laser Fluorescence Angiography with Indocyanine Green Predicts Early Graft Function after Kidney Transplantation. Annals of Surgery Publish Ahead of Print. 2020;30:30.
10. Girard N, Delomenie M, Malhaire C, Sebbag D, Roulot A, Sabaila A, et al. Innovative DIEP flap perfusion evaluation tool: Qualitative and quantitative analysis of indocyanine green-based fluorescence angiography with the SPY-Q proprietary software. PLoS One. 2019;14(6):e0217698.
11. Mironov O, Zener R, Eisenberg N, Tan KT, Roche-Nagle G. Real-Time Quantitative Measurements of Foot Perfusion in Patients With Critical Limb Ischemia. Vasc Endovascular Surg. 2019;53(4):310-5.
12. Regus S, Klingler F, Lang W, Meyer A, Almasi-Sperling V, May M, et al. Pilot study using intraoperative fluorescence angiography during arteriovenous hemodialysis access surgery. Journal of Vascular Access. 2019;20(2):175-83.
13. Rother U, Muller-Mohnssen H, Lang W, Ludolph I, Arkudas A, Horch RE, et al. Wound closure by means of free flap and arteriovenous loop: Development of flap autonomy in the long-term follow-up. International Wound Journal. 2020;17(1):107-16.

14. Rother U, Amann K, Adler W, Nawroth N, Karampinis I, Keese M, et al. Quantitative assessment of microperfusion by indocyanine green angiography in kidney transplantation resembles chronic morphological changes in kidney specimens. Microcirculation. 2019;26(3):e12529.
15. Rother U, Lang W, Horch RE, Ludolph I, Meyer A, Gefeller O, et al. Pilot Assessment of the Angiosome Concept by Intra-operative Fluorescence Angiography After Tibial Bypass Surgery. European Journal of Vascular and Endovascular Surgery. 2018;55(2):161.
16. Rother U, Lang W, Horch RE, Ludolph I, Meyer A, Regus S. Microcirculation Evaluated by Intraoperative Fluorescence Angiography after Tibial Bypass Surgery. Annals of Vascular Surgery. 2017;40:190-7.
17. Yang CE, Chung SW, Lee DW, Lew DH, Song SY. Evaluation of the Relationship Between Flap Tension and Tissue Perfusion in Implant-Based Breast Reconstruction Using Laser-Assisted Indocyanine Green Angiography. Ann Surg Oncol. 2018;25(8):2235-40.
18. Colvard B, Itoga NK, Hitchner E, Sun Q, Long B, Lee G, et al. SPY technology as an adjunctive measure for lower extremity perfusion. J Vasc Surg. 2016;64(1):195-201.
19. Fichter AM, Ritschl LM, Georg R, Kolk A, Kesting MR, Wolff KD, et al. Effect of Segment Length and Number of Osteotomy Sites on Cancellous Bone Perfusion in Free Fibula Flaps. Journal of Reconstructive Microsurgery. 2019;35(2):108-16.
20. Kang Y, Lee J, Kwon K, Choi C. Application of novel dynamic optical imaging for evaluation of peripheral tissue perfusion. International Journal of Cardiology. 2010;145(3):e99-101.
21. Hajhosseini B, Chiou GJ, Virk SS, Chandra V, Moshrefi S, Meyer S, et al. Hyperbaric Oxygen Therapy in Management of Diabetic Foot Ulcers: Indocyanine Green Angiography May Be Used as a Biomarker to Analyze Perfusion and Predict Response to Treatment. Plast Reconstr Surg. 2021;147(1):209-14.
22. Han MD, Miloro M, Markiewicz MR. Laser-Assisted Indocyanine Green Imaging for Assessment of Perioperative Maxillary Perfusion During Le Fort I Osteotomy: A Pilot Study. J Oral Maxillofac Surg. 2018;76(12):2630-7.
23. Hitier M, Cracowski JL, Hamou C, Righini C, Bettega G. Indocyanine green fluorescence angiography for free flap monitoring: A pilot study. J Craniomaxillofac Surg. 2016;44(11):1833-41.
24. Lang BHH, Wong CKH, Hung HT, Wong KP, Mak KL, Au KB. Indocyanine green fluorescence angiography for quantitative evaluation of in situ parathyroid gland perfusion and function after total thyroidectomy. Surgery (United States). 2017;161(1):87-95.
25. Son GM, Kwon MS, Kim Y, Kim J, Kim SH, Lee JW. Quantitative analysis of colon perfusion pattern using indocyanine green (ICG) angiography in laparoscopic colorectal surgery. Surg Endosc. 2019;33(5):1640-9.
26. Amagai H, Miyauchi H, Muto Y, Uesato M, Ohira G, Imanishi S, et al. Clinical utility of transanal indocyanine green near-infrared fluorescence imaging for evaluation of colorectal anastomotic perfusion. Surg Endosc. 2020;34(12):5283-93.
27. Goertz L, Hof M, Timmer M, Schulte AP, Kabbasch C, Krischek B, et al. Application of Intraoperative FLOW 800 Indocyanine Green Videoangiography Color-Coded Maps for Microsurgical Clipping of Intracranial Aneurysms. World Neurosurg. 2019;131:e192-e200.

28. Hayami S, Matsuda K, Iwamoto H, Ueno M, Kawai M, Hirono S, et al. Visualization and quantification of anastomotic perfusion in colorectal surgery using near-infrared fluorescence. Tech Coloproctol. 2019;23(10):973-80.
29. Igari K, Kudo T, Toyofuku T, Jibiki M, Inoue Y, Kawano T. Quantitative Evaluation of the Outcomes of Revascularization Procedures for Peripheral Arterial Disease Using Indocyanine Green Angiography. European Journal of Vascular & Endovascular Surgery. 2013;46(4):460-5.
30. Igari K, Kudo T, Uchiyama H, Toyofuku T, Inoue Y. Indocyanine Green Angiography for the Diagnosis of Peripheral Arterial Disease with Isolated Infrapopliteal Lesions. Annals of Vascular Surgery. 2014;28(6):1479-84.
31. Ishige F, Nabeya Y, Hoshino I, Takayama W, Chiba S, Arimitsu H, et al. Quantitative Assessment of the Blood Perfusion of the Gastric Conduit by Indocyanine Green Imaging. J Surg Res. 2019;234:303-10.
32. Kamiya K, Unno N, Miyazaki S, Sano M, Kikuchi H, Hiramatsu Y, et al. Quantitative assessment of the free jejunal graft perfusion. Journal of Surgical Research. 2015;194(2):394-9.
33. Kamp MA, Sarikaya-Seiwert S, Petridis AK, Beez T, Cornelius JF, Steiger HJ, et al. Intraoperative Indocyanine Green-Based Cortical Perfusion Assessment in Patients Suffering from Severe Traumatic Brain Injury. World Neurosurg. 2017;101:431-43.
34. Kamp MA, Slotty P, Turowski B, Etminan N, Steiger HJ, Hanggi D, et al. Microscope-integrated quantitative analysis of intraoperative indocyanine green fluorescence angiography for blood flow assessment: first experience in 30 patients. Neurosurgery. 2012;70(1 Suppl Operative):65-73; discussion -4.
35. Kobayashi S, Ishikawa T, Tanabe J, Moroi J, Suzuki A. Quantitative cerebral perfusion assessment using microscope-integrated analysis of intraoperative indocyanine green fluorescence angiography versus positron emission tomography in superficial temporal artery to middle cerebral artery anastomosis. Surg Neurol Int. 2014;5:135.
36. Maxwell AK, Deleyiannis FW. Utility of Indocyanine Green Angiography in Arterial Selection during Free Flap Harvest in Patients with Severe Peripheral Vascular Disease. Plast Reconstr Surg Glob Open. 2016;4(10):e1097.
37. Miyazaki H, Igari K, Kudo T, Iwai T, Wada Y, Takahashi Y, et al. Significance of the Lateral Thoracic Artery in Pectoralis Major Musculocutaneous Flap Reconstruction: Quantitative Assessment of Blood Circulation Using Indocyanine Green Angiography. Ann Plast Surg. 2017;79(5):498-504.
38. Nakamura M, Igari K, Toyofuku T, Kudo T, Inoue Y, Uetake H. The evaluation of contralateral foot circulation after unilateral revascularization procedures using indocyanine green angiography. Scientific Reports. 2017;7.
39. Nishizawa M, Igari K, Kudo T, Toyofuku T, Inoue Y, Uetake H. A Comparison of the Regional Circulation in the Feet between Dialysis and Non-Dialysis Patients using Indocyanine Green Angiography. Scandinavian Journal of Surgery. 2017;106(3):249-54.
40. Patel HM, Bulsara SS, Banerjee S, Sahu T, Sheorain VK, Grover T, et al. Indocyanine Green Angiography to Prognosticate Healing of Foot Ulcer in Critical Limb Ischemia: A Novel Technique. Ann Vasc Surg. 2018;51:86-94.

41. Rennert RC, Strickland BA, Ravina K, Bakhsheshian J, Russin JJ. Assessment of Hemodynamic Changes and Hyperperfusion Risk After Extracranial-to-Intracranial Bypass Surgery Using Intraoperative Indocyanine Green-Based Flow Analysis. World Neurosurg. 2018;114:352-60.
42. Schneider P, Piper S, Schmitz CH, Schreiter NF, Volkwein N, Ludemann L, et al. Fast 3D Near-infrared breast imaging using indocyanine green for detection and characterization of breast lesions. Rofo: Fortschritte auf dem Gebiete der Rontgenstrahlen und der Nuklearmedizin. 2011;183(10):956-63.
43. Seinturier C, Blaise S, Tiffet T, Provencher CB, Cracowski JL, Pernod G, et al. Fluorescence angiography compared to toe blood pressure in the evaluation of severe limb ischemia. Vasa. 2020;49(3):230-4.
44. Settembre N, Kauhanen P, Alback A, Spillerova K, Venermo M. Quality Control of the Foot Revascularization Using Indocyanine Green Fluorescence Imaging. World J Surg. 2017;41(7):1919-26.
45. Shi W, Qiao G, Sun Z, Shang A, Wu C, Xu B. Quantitative assessment of hemodynamic changes during spinal dural arteriovenous fistula surgery. J Clin Neurosci. 2015;22(7):1155-9.
46. Tanaka K, Okazaki M, Yano T, Miyashita H, Homma T, Tomita M. Quantitative evaluation of blood perfusion to nerves included in the anterolateral thigh flap using indocyanine green fluorescence angiography: a different contrast pattern between the vastus lateralis motor nerve and femoral cutaneous nerve. J Reconstr Microsurg. 2015;31(3):163-70.
47. Wada T, Kawada K, Takahashi R, Yoshitomi M, Hida K, Hasegawa S, et al. ICG fluorescence imaging for quantitative evaluation of colonic perfusion in laparoscopic colorectal surgery. Surg Endosc. 2017;31(10):4184-93.
48. Ye X, Liu XJ, Ma L, Liu LT, Wang WL, Wang S, et al. Clinical values of intraoperative indocyanine green fluorescence video angiography with Flow 800 software in cerebrovascular surgery. Chin Med J (Engl). 2013;126(22):4232-7.
49. Zhang X, Ni W, Feng R, Li Y, Lei Y, Xia D, et al. Evaluation of Hemodynamic Change by Indocyanine Green-FLOW 800 Videoangiography Mapping: Prediction of Hyperperfusion Syndrome in Patients with Moyamoya Disease. Oxidative Medicine and Cellular Longevity. 2020;2020 (no pagination).
50. Zimmermann A, Roenneberg C, Reeps C, Wendorff H, Holzbach T, Eckstein HH. The determination of tissue perfusion and collateralization in peripheral arterial disease with indocyanine green fluorescence angiography. Clin Hemorheol Microcirc. 2012;50(3):157-66.
51. Mothes H, Dinkelaker T, DÖNicke T, Friedel R, Hofmann GO, Bach O. Outcome Prediction in Microsurgery by Quantitative Evaluation of Perfusion Using ICG Fluorescence Angiography. J Hand Surg Eur Vol. 2009;34(2):238-46.
52. Betz CS, Zhorzel S, Schachenmayr H, Stepp H, Havel M, Siedek V, et al. Endoscopic measurements of free-flap perfusion in the head and neck region using red-excited Indocyanine Green: preliminary results. J Plast Reconstr Aesthet Surg. 2009;62(12):1602-8.
53. Betz CS, Zhorzel S, Schachenmayr H, Stepp H, Matthias C, Hopper C, et al. Endoscopic assessment of free flap perfusion in the upper aerodigestive tract using indocyanine green: a pilot study. J Plast Reconstr Aesthet Surg. 2013;66(5):667-74.

54. Aiba T, Uehara K, Ogura A, Tanaka A, Yonekawa Y, Hattori N, et al. The significance of the time to arterial perfusion in intraoperative ICG angiography during colorectal surgery. Surg Endosc. 2021.
55. Kang Y, Lee J, An Y, Jeon J, Choi C. Segmental analysis of indocyanine green pharmacokinetics for the reliable diagnosis of functional vascular insufficiency. J Biomed Opt. 2011;16(3):030504.
56. D'Urso A, Agnus V, Barberio M, Seeliger B, Marchegiani F, Charles AL, et al. Computer-assisted quantification and visualization of bowel perfusion using fluorescence-based enhanced reality in left-sided colonic resections. Surgical Endoscopy. 2020.
57. Gorai K, Inoue K, Saegusa N, Shimamoto R, Takeishi M, Okazaki M, et al. Prediction of Skin Necrosis after Mastectomy for Breast Cancer Using Indocyanine Green Angiography Imaging. Plast Reconstr Surg Glob Open. 2017;5(4):e1321.
58. Prinz V, Hecht N, Kato N, Vajkoczy P. FLOW 800 allows visualization of hemodynamic changes after extracranial-to-intracranial bypass surgery but not assessment of quantitative perfusion or flow. Neurosurgery. 2014;10 Suppl 2:231-8; discussion 8-9.
59. Rennert RC, Strickland BA, Ravina K, Brandel MG, Bakhsheshian J, Fredrickson V, et al. Assessment of ischemic risk following intracranial-to-intracranial and extracranial-to-intracranial bypass for complex aneurysms using intraoperative Indocyanine Green-based flow analysis. J Clin Neurosci. 2019;67:191-7.
60. Terasaki H, Inoue Y, Sugano N, Jibiki M, Kudo T, Lepantalo M, et al. A quantitative method for evaluating local perfusion using indocyanine green fluorescence imaging. Ann Vasc Surg. 2013;27(8):1154-61.
61. Holling M, Brokinkel B, Ewelt C, Fischer BR, Stummer W. Dynamic ICG fluorescence provides better intraoperative understanding of arteriovenous fistulae. Neurosurgery. 2013;73(1 Suppl Operative):ons93-8; discussion ons9.
62. Woitzik J, Pena-Tapia PG, Schneider UC, Vajkoczy P, Thome C. Cortical perfusion measurement by indocyanine-green videoangiography in patients undergoing hemicraniectomy for malignant stroke. Stroke. 2006;37(6):1549-51.
63. Uchino H, Nakamura T, Houkin K, Murata JI, Saito H, Kuroda S. Semiquantitative analysis of indocyanine green videoangiography for cortical perfusion assessment in superficial temporal artery to middle cerebral artery anastomosis. Acta Neurochirurgica. 2013;155(4):599-605.
64. Uchino H, Kazumata K, Ito M, Nakayama N, Kuroda S, Houkin K. Intraoperative assessment of cortical perfusion by indocyanine green videoangiography in surgical revascularization for moyamoya disease. Acta Neurochir (Wien). 2014;156(9):1753-60.
65. Venermo M, Settembre N, Alback A, Vikatmaa P, Aho PS, Lepantalo M, et al. Pilot Assessment of the Repeatability of Indocyanine Green Fluorescence Imaging and Correlation with Traditional Foot Perfusion Assessments. European Journal of Vascular & Endovascular Surgery. 2016;52(4):527-33.
66. Lutken CD, Achiam MP, Svendsen MB, Boni L, Nerup N. Optimizing quantitative fluorescence angiography for visceral perfusion assessment. Surgical Endoscopy. 2020;34(12):5223-33.
67. Nerup N, Andersen HS, Ambrus R, Strandby RB, Svendsen MBS, Madsen MH, et al. Quantification of fluorescence angiography in a porcine model. Langenbecks Arch Surg. 2017;402(4):655-62.

68. Rønn JH, Nerup N, Strandby RB, Svendsen MBS, Ambrus R, Svendsen LB, et al. Laser speckle contrast imaging and quantitative fluorescence angiography for perfusion assessment. Langenbecks Arch Surg. 2019;404(4):505-15.
69. Lutken CD, Achiam MP, Osterkamp J, Svendsen MB, Nerup N. Quantification of fluorescence angiography: Toward a reliable intraoperative assessment of tissue perfusion - A narrative review. Langenbecks Archives of Surgery. 2020;21:21.